Available online at www.sciencedirect.com
SCIENCE DIRECT
ELSEVIER
Polymer 46 (2005) 2244–2256
polymer
www.elsevier.com/locate/polymer

Mechanical properties of PP-LDPE blends with novel morphologies produced with a continuous chaotic advection blender

A. Dhoble, B. Kulshreshtha, S. Ramaswami, D.A. Zumbrunnen*

Department of Mechanical Engineering and the School of Materials Science & Engineering, 214 Fluor Daniel Building, Clemson University, Clemson, SC 29634-0921, USA

Received 18 October 2004; received in revised form 12 January 2005; accepted 20 January 2005

Abstract

When immiscible polymer melts are combined by chaotic advection, melt domains are recursively stretched and folded. A multi-layer blend morphology results that has a hierarchical structure and intrinsic mechanical interlocking. Novel derivative morphologies can be obtained via the formation and interactive growth of holes among melt layers. In this study, a unique continuous chaotic advection blender (CCAB) was used to investigate influences of these morphologies on tensile and impact toughness properties of polypropylene (PP)-low density polyethylene (LDPE) blends. Although prior related work has focused on batch processing, this study also demonstrated the viability of chaotic advection in continuous flow modes suited for extruding blends with target morphologies. Extrusions were producible with morphologies giving an overall combination of improved properties relative to properties associated with droplet morphologies typically obtained with conventional compounding equipment. Applicability to injection molding is also discussed. Novel processing control features of the CCAB-type devices are briefly described.

Keywords: Polypropylene; Blends; Chaotic mixing

1. Introduction

Due to polymer immiscibility, the physical properties of many polymer blends derive from the fine-scale structural arrangements, or blend morphologies, obtained during processing in addition to the proportion of each polymer type present. Interestingly, most immiscible polymer blends are produced by mixing in sharp contrast to many other types of composite materials where methods are designed to deliberately form material components into functional shapes and place them in structures associated with property enhancements. Because mixing constrains the variety of morphologies producible, many immiscible polymer blends are not necessarily optimized with regard to structure, composition, and properties. Technologies such as co-extrusion have been developed to obtain structured plastic materials such as low permeation films. However, methods to create directly functional structures in immiscible polymer blends in compounding steps are less developed.

Chaotic advection [1,2] has been proposed as a method to more controllably build in situ specific blend morphologies [3–8]. Chaotic advection involves the recursive stretching and folding of melt domains in response to shear flows that can be comparatively much simpler than flows occurring in conventional compounding equipment. (The term, chaotic mixing, is also used but the parent term is deemed more appropriate where in situ structuring is a focus.) As a consequence, melts become organized into expansive layers of decreasing thickness and increasing number. Blends have been produced in polymer systems having very low interfacial tension with individual layer thicknesses as small as 5–10 nm, although layer thicknesses of several hundred nanometers are typical of many immiscible polymer blends [9,10] Patterns evolved in fluids from chaotic advection are hierarchical [11]. This hierarchical arrangement among polymer melt layers can provide a useful mechanical interlocking in plastics to offset poor

* Corresponding author. Tel.: +1 864 656 5625; fax: +1 864 656 4435.
E-mail address: zdavid@ces.clemson.edu (D.A. Zumbrunnen).

0032-3861/$ - see front matter © 2005 Elsevier Ltd. All rights reserved.
doi:10.1016/j.polymer.2005.01.057

interfacial adhesion typifying interfaces between immiscible polymers [12]. Due to interfacial instabilities that occur, the multi-layer morphology serves as a parent morphology to derivative blend morphologies. Gradual refinement in the layers promotes progressive morphology development and allows sequential morphology transitions [6]. Many of the derivative morphologies are also novel and some provide interconnections between polymer components. Examples include multiple layers interconnected via holes of selectable average size, co-continuous phases formed with reduced restrictions on composition, platelets and ribbons distributed volumetrically, abundant fibers of large length, and small droplets with diameters related to parent layer thickness [7–9].

Hierarchical structures if producible in plastics can give intrinsic increases in toughness. Increases may arise due to localized failures occurring initially within the smallest internal portions of a hierarchical structure [13]. In consideration of the hierarchical and interlocked morphologies in immiscible blends resulting from chaotic advection in prior investigations, a compelling rationale arose for the study documented in this paper. Although extensively used, the application of polypropylene (PP) has been hindered by relatively low impact toughness especially at low temperatures [14,15]. It was, therefore, selected for this study as an appropriate major component polymer. Some degree of success has been achieved in modification of PP using rubber additives [16–21], but noticeable reductions in stiffness and scratch/mar resistance can occur in the resulting blends [22]. Blends of PP and low density polyethylene (LDPE) may give a better balance between toughness improvements and stiffness reductions. The unique continuous chaotic advection blender (CCAB) that was employed in this investigation allowed production of PP-LDPE blends having a wide variety of morphologies even at low LDPE volume compositions. The CCAB permitted independent assessments of morphology and compositional effects on mechanical properties. For example, the various morphologies were producible at each composition. This capability is novel and is discussed in further detail below. Screw extruders, in contrast, yield only droplet morphologies at these low compositions with no mechanical interlocking so morphology effects are largely unreported.

Melts of PP and LDPE are immiscible and form blends having low interfacial adhesion [23]. Droplets of LDPE as a soft rubbery phase improved the impact resistance of PP by promoting crazing and thereby absorbing impact energy. Because of low interfacial adhesion, compatibilizers are often added such as ethylene–propylene block copolymer also known as ethylene–propylene rubber. Chiu and Fang [24] blended PP and LDPE and added ethylene–propylene copolymer (either random or block) to improve interfacial adhesion. The impact strength of the blend with the random copolymer was larger by a factor of six than the impact strength of PP, while the block copolymer provided a factor of three. For uncompatibilized PP-LDPE blends considered in this paper, pronounced crazing and improved toughness have been observed when the average diameter of dispersed LDPE droplets is less than about 0.5 μm [15,20]. In a comparative study, Tai et al. [19] blended PP with 20% LDPE or 20% HDPE using a single screw extruder. The impact strength of PP was reduced by the addition of HDPE but was marginally improved by LDPE. LDPE droplets decreased the spherulite size and ultimate tensile strength of PP. Lu et al. [25] suggested that as long as a second phase polymer can generate numerous stress concentration sites lateral to a crack tip and relieve tri-axial tensile stresses, a brittle matrix can be toughened by a dispersed second phase polymer.

One prior study investigated the mechanical properties of blends resulting from chaotic advection. A batch chaotic advection blending device was designed [26], implemented in a morphology study [3], and later used to study blend morphology effects on the impact toughnesses of blends composed of polystyrene (PS) and 9% by mass LDPE [5]. Castings were obtained with multi-layer, abundant long fiber, and droplet morphologies present in differing proportions related to the processing time. A predominant fiber morphology enhanced impact toughness by 69% relative to the toughness for the droplet morphology. This early work suggested that droplet morphologies typically obtained at low compositions by conventional blending methods may not be the most favorable for impact toughness improvements.

In the following sections, the operation of the CCAB is described. Many operating features are novel, such as capabilities to produce extrusions with a specific target morphology or with morphologies changing periodically along an extrusion length. (Because blend morphology can be dynamically controlled on-line and particular blend morphologies are essentially constructed in situ, CCAB devices are also known as ‘smart blenders’). The CCAB was implemented to produce PP-LDPE films extruded with thicknesses of 150 μm and 500 μm at compositions of 10, 20, and 30% by volume. Several blend morphologies were produced in films at each composition. Tensile and impact properties of the films are presented in terms of a CCAB process control parameter related directly to morphology. Taken together with micrographs of various blend morphologies produced, mechanical properties are related directly to blend morphology by reference to the same parameter. While PP-LDPE blends are of general interest, this paper also demonstrates how CCAB devices can be implemented in structure-property-composition studies.

2. Experimental procedures

2.1. Description of continuous chaotic advection blender

The CCAB is shown schematically in Fig. 1. LDPE and

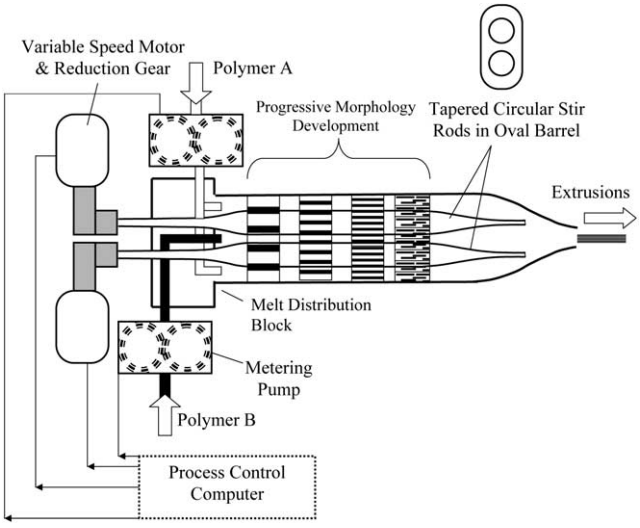

Fig. 1. Schematic representation of the continuous chaotic advection blender (CCAB).

PP melts were supplied by metering pumps at prescribed volumetric flow rates to yield blends of desired composition. Each metering pump was fed by a single screw extruder (1.905 cm, $L/D=24$) operated in a constant discharge pressure mode. Melt from the metering pumps entered the CCAB via a cylindrical melt distribution block. The block contained nine, 0.6 cm ports for the minor component LDPE (polymer A) located with equal spacing along the circumference and one central 1.0 cm diameter port for the PP melt (polymer B). The CCAB barrel had circular inner profiles at both ends, which quickly transitioned to an oval cross-section over the mid-span. Its overall length was 30 cm. Chaotic advection (Section 2.2) was instilled by two 59.5 cm long stir rods placed 1.5 cm offset from the barrel axis. The rods were rotated by variable speed motors that were independently controllable via a computer interface. The rods were flared to a 2.22 cm diameter within the oval barrel cross-section and were tapered within the circular transition portions. The rod tapering in the vicinity of the distribution block precluded physical interference between the melt injection ports and the portion of the stir rods extending to the drive motors. Tapering adjacent to the die provided a hydrodynamic transition in order to convey the structured melt with minimal disturbances from the CCAB barrel.

Blends were extruded as films using one of two dies. The use of different dies allowed assessment of die effects on morphologies produced. One die provided films of 500 μ thickness and 10.2 cm width. The other provided films of 150 μ thickness and 23 cm width. Each die had a simultaneous linear taper and transverse expansion. Other dies can also be fitted onto the CCAB to produce extrusions of other forms. For example, prior published work has shown that similar morphologies can be captured in extrusions produced with filament or film dies [9,10,12,27]. The extruded films were solidified on a chill roll maintained at 20 °C and wound onto a spool. An automated heating system with independent temperature zones maintained the CCAB and attached die at the selected processing temperature.

2.2. Process control and definition of CCAB parameter N

Requisite conditions for inducing chaotic advection in driven flows have been widely studied [28–31]. Due to a pressure-driven axial flow and rod-driven circumferential flow in the CCAB of Fig. 1, the flow field was three-dimensional. However, the simple geometry of the stir rods instilled chaotic advection principally within planes parallel to the cross section of the CCAB barrel. The extent of melt structuring along the barrel by progressive morphology development [6,8,12] was selectable via specification of a number N denoting pairs of rod rotational speed changes while melt was resident in the CCAB. To clearly define N, let one rod in Fig. 1 be designated as R_1, the other rod be designated as R_2, and Ω denote the number of rotations for a designated rod. For added generality, counter-clockwise rotations are given by $\Omega<0$ and clockwise rotations are given by $\Omega>0$. In terms of these parameters, designation of R_1 rotating three complete rotations and R_2 rotating simultaneously one complete rotation is denoted by $[R_1(\Omega=3)+R_2(\Omega=1)]$. A specific rod rotational protocol for the CCAB consisted of a periodic sequence of rod motions. In this study, this sequence consisted of N repetitions of the rod motions given by $[R_1(\Omega=3)+R_2(\Omega=1);\ R_1(\Omega=1)+R_2(\Omega=3)]$. For example, for $N=3$, rod rotations occurred according to $[R_1(\Omega=3)+R_2(\Omega=1);R_1(\Omega=1)+R_2(\Omega=3)];[R_1(\Omega=3)\ \ R_2(\Omega=1);\ \ R_1(\Omega=1)+R_2(\Omega=3)];\quad R_1(\Omega=3)+R_2(\Omega=1);\quad R_1(\Omega=1)+R_2(\Omega=3)]$. For a selected extrusion rate, rod speed is selected such that the desired value of N can be obtained while melt is resident in the CCAB.

The effectiveness of the rod rotational protocol to yield chaotic advection throughout the blender volume was evaluated computationally and also experimentally in a procedure analogous to those employed in chaotic mixing studies such as those previously cited. In the experimental evaluations, a pigmented thermoplastic or a masterbatch of carbon black and thermoplastic was supplied as the polymer B melt in Fig. 1 while the identical non-pigmented thermoplastic was supplied as the matrix polymer A. The uniformity of the pigmented component or carbon black in extrusions was examined by optical microscopy for candidate rod rotational protocols. The selected protocol above of simple periodic rod motion led to the eventual redistribution throughout the extrusion cross-sections of the injected pigmented thermoplastic or carbon black. In computational simulations [32], velocity fields were evaluated by a finite element method and were used to track advected particle positions and construct Poincarè sections. Similar methods were employed in the design of a batch chaotic advection blender [26] and chaotic mixing studies

[29–31]. Global chaotic advection was indicated by the redistribution of particles throughout the CCAB volume and an absence of elliptic (non-chaotic) regions larger than about 1% of the CCAB flow cross-sectional area for $N>5$. An example of the computational results is given in Fig. 2. Six clusters of particles ($N=0$) and a major component were increasingly redistributed throughout the CCAB cross-section as N increased. The particle clusters and major component were stretched and folded about the other to give alternating layers with thicknesses decreasing with N. In actual polymer melts, minor components are continuous phases in lieu of discrete particles. As such and in consideration of the cross-sectional view, numerous continuous layers arise in lieu of the granular patterns of Fig. 2. The multi-layer morphology serves as a parent morphology to derivative morphologies. Morphology transitions have been studied computationally [34] and results are in good agreement with blend morphology development reported in this paper.

The CCAB provided considerable operational flexibility in controlling morphology development. As described earlier, the recursive stretching and folding of melt domains is a defining characteristic of chaotic advection. This characteristic is represented in Fig. 1 by the alternating black and white bands in the vicinity of the stir rods. Upon entering the CCAB, the PP and LDPE melt components were initially configured according to the hole pattern in the melt distribution block. By injecting the melts as large diameter streams, interfacial tension forces were reduced initially so minor components even of relatively high viscosity were readily deformed in the very low Reynolds number flow. Because stretching and folding caused interfacial areas to increase, subsequent deformation and refinement of layers were more easily achieved by imposed shear than the initial deformations [8,33]. Transformation of injected melts into layers also prevented fragmentation by capillary instabilities. Interfacial tension in a layer, for example, will resist indentation so conversion of melts to layers by chaotic advection forestalls breakup and provides good component redistribution and size reduction. Extrusions can be obtained with few thick layers or with numerous thin layers by selecting a stir rod rotational speed and displacement to impart the needed amount of melt structuring in terms of N while the melt is resident in the CCAB. As will be shown, other morphologies can also be obtained from eventual breakup of the multiple layers by increasing melt residence time further [6]. It can be anticipated from Fig. 2 that extrusions with $N<3$ from the CCAB may have considerable property variability due to partial component redistribution.

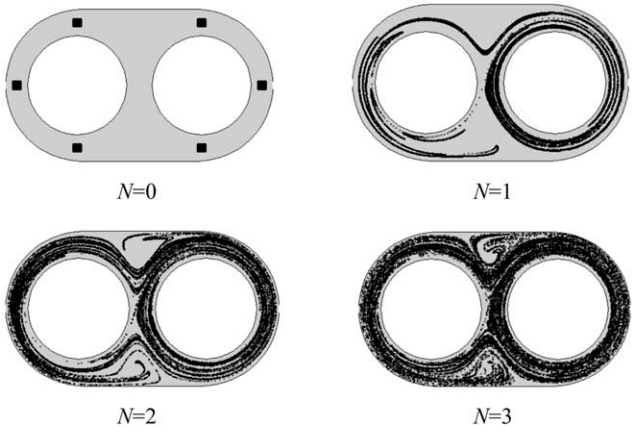

Fig. 2. Computational simulation of distribution by chaotic advection of initial minor component melt bodies (black squares) into a major component melt (gray) in response to the rod rotational protocol used with the CCAB of Fig. 1 [32].

By careful consideration of these methods, blend morphology appearing in an extrusion can be made to change dynamically. For example, if rod speed is reduced and melt flow is continued, multiple, thin layers in an extrusion become progressively less numerous and thicker, or a droplet morphology can revert to its parent fibrous or multi-layer morphology. More generally, rod rotational speed and metering pump flow rates can be adjusted to change N and perform on-line optimization of properties, structure, and composition. In general, the CCAB can be operated in two unsteady modes. In a dynamic mode, CCAB operation (e.g. melt flow rates, rod rotational protocol) is changed repeatedly or continuously. In this study, the transient mode was used. For the transient mode, a single change is made to CCAB operation so an initial structure in an extrusion transforms over time to a subsequent one. LDPE and PP melts were steadily injected while the stir rods were stationary. LDPE and PP bands, or streaks, appeared steadily in the extrusion that resembled their injection pattern from the melt distribution block (Fig. 1). Stir rod motion was started in accordance with the protocol defined above to initiate chaotic advection and begin in situ structuring. Rotational speeds of 6 RPM and 2 RPM corresponded to $\Omega=3$ and $\Omega=1$, respectively. Under these conditions, melt in the CCAB barrel that was located nearer to the die had a smaller residence time and underwent less structuring than melt closer to the melt distribution block. Collected film was obtained with increasing amounts of structuring along its length until steady-state conditions were reached. Steady state corresponded to the value of N for the melt residence time in the CCAB. For the chosen rod rotational speeds and metering pump flow rates, blends with $N=20$ had melt residence times of 20 min while blends with smaller N had melt residence times that were proportionally smaller. The melt residence times of this study were consequences of the installed metering pump ratings. Metering pumps with higher melt flow rates may allow higher extrusion rates.

2.3. Materials used and their rheological properties

Blends were produced of polypropylene and low density polyethylene (PP H701-20A, LDPE 4012, Dow Chemical

Company, Midland, Michigan) in volume compositions of 10, 20 and 30% LDPE. The PP and LDPE had melt flow indices (g/min, ASTM D1238) of 20 and 12, respectively. The shear viscosities of PP and LDPE were determined at candidate processing temperatures using a cone and plate rheometer (Rheometric Scientific, ARES, Piscataway, NJ). Results are given in Fig. 3. For the applicable shear rates in the CCAB of Fig. 1 ranging from 0.5 to 1.5/s, a processing temperature of 230 °C was selected and provided a viscosity ratio C_μ between 1.4 and 1.7. Due to the low shear rates and machine-induced deformations in the CCAB occurring in response to flow fields that remained steady over intervals spanning tens of seconds, the Weissenberg number was small. For these processing conditions, C_μ and interfacial tension σ were primary melt properties. Morphology development occurs more slowly at higher viscosity ratios while early layer breakup at low viscosity ratios can reduce selectivity through process parameter specification of blend morphology types [7,33]. Viscosity ratios of about unity for the PP-LDPE blends provided conditions where LDPE layers formed readily, became well distributed throughout the CCAB barrel, and attained sub-micron thicknesses.

2.4. Microscopy, tensile and impact tests

For documentation of various blend morphologies, film samples corresponding to different N were examined by low voltage scanning electron microscopy (LV SEM, Hitachi, Model S4700, Tokyo, Japan). In addition to using LV SEM, sample preparation procedures were developed to further improve contrast between the PP and LDPE components. Collected films were immersed in liquid nitrogen for 5 min or longer. Immediately afterward, the films were fractured in either the transverse or machine directions (i.e., across the film width or along the film length) to provide orthogonal perspectives of developed morphologies. Contrast was derived chiefly from differing textures of domains in fracture surfaces pertaining to each polymer component and also by revealing morphology features via delamination

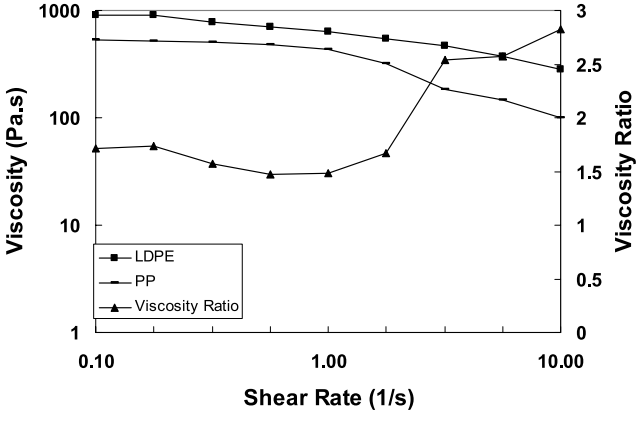

Fig. 3. Viscosities and viscosity ratio for LDPE and PP at the processing temperature of 230 °C.

resulting from poor interfacial adhesion between the immiscible polymer pair. The effectiveness of this approach was validated by comparing images obtained by the above procedure with those obtained with samples subjected to dissolution using selective solvents in prior and ongoing studies with the CCAB and batch chaotic advection blenders. Blend morphology was documented in terms of N for $0<N<20$ to disclose progressive morphology development. By inspecting micrographs for integer or fractional values of N, methods allowed detailed investigations of morphology transition mechanisms. To assess morphology uniformity, films were also examined at different locations along the film width and across the film thickness.

Tensile tests were performed according to ASTM D-882 by cutting five rectangular specimens from films produced with the 500 μm die both in the machine and transverse directions. An Instron tensile testing machine (Model T 10000, SATEC Systems, Grove City, PA) was used with a gauge length of 5.1 cm and crosshead speed of 1.27 cm/min. ASTM D-882 specifies a test specimen width between 5 mm and 25.4 mm and a width-to-thickness ratio of at least 8. Accordingly, specimens of 12.7 mm width were used.

Because blends were extruded as films, impact tests were carried out using a dart drop impact tester (DDI/TE, Model DDI-120, Qualitest Inc., Fort Lauderdale, Florida, USA) in accordance with ASTM D-4272. Films for impact testing were produced with the 150 μm film die. A 38.1 mm dart was used. Five specimens were tested for each N and an average impact energy was calculated. The impact energy was based on the difference in kinetic energy of the falling dart after passing through a clamped film sample relative to the kinetic energy of the dart after traversing an identical vertical distance in free fall.

3. Results and discussion

3.1. Description of blend morphologies

In figures which follow, blend morphologies are presented in terms of the process parameter N (Section 2.2) indicating the amount of imposed melt structuring with the CCAB of Fig. 1 in response to stir rod motion. Each figure pertains to a specific N and includes morphologies for the three LDPE volume compositions of 10, 20, and 30%. Progressive morphology development can be discerned by sequentially inspecting micrographs of each figure corresponding to a particular composition. As discussed in relation to Fig. 1, the PP and LDPE were injected as continuous streams that became subjected to the stretching and folding characteristic of chaotic advection. Both the PP and LDPE were converted to layers and became mutually enveloped such that a hierarchical arrangement arose. The progression of stretching, folding, and envelopment as melt moved along the CCAB barrel led to improved

compositional uniformity over decreasing length scales. Examples of the multi-layer morphologies are given in Fig. 4 for $N=8$. LDPE layer thicknesses were less than 0.5 μm at all compositions. The relative thicknesses of the LDPE and PP layers were on average equal to the blend composition as with any layered configuration. Extruded films for smaller N had fewer and thicker layers. Methods thereby permitted extrusion of blends having a selectable average layer thickness and layer number. Similar layer formation by chaotic advection has been documented with batch devices [3–5,8] and previously in an early CCAB prototype [9,12,27].

In immiscible melts organized into multiple layers by chaotic advection, layer breakup has been shown experimentally and computationally to occur volumetrically via the formation and growth of holes [7,8,34]. Layer formation, hole growth, and layer fragmentation have also been used to describe how resin pellets in twin screw extruders break quickly into small shapes [35]. In contrast to localized and uncontrollable breakup, melt components were organized in the CCAB into expansive multiple layers such that holes grew volumetrically and, at intermediate compositions, also interactively via melt redistribution among the layers in response to enlarging holes. Particular shapes in a minor component arose and in some cases all together new blend morphologies were produced. In essence, by organizing melts in lieu of dispersing them, chaotic advection permitted selection and promotion of a particular blend morphology that may be transitory and localized in conventional blending equipment. Examples of layers undergoing morphology transitions are given in Fig. 5 for $N=10$. The transitions were qualitatively similar at the 10 and 20% LDPE compositions while the transition for the 30% case differed markedly. For the 10 and 20% LDPE blends, interlayer spacing was sufficient to allow LDPE layers to behave as essentially autonomous layers. For example, hole formation and growth in each LDPE layer led to the formation of discrete LDPE bodies without coalescence between LDPE of different layers. The circular domains in the transverse views of Fig. 5a and b were fibers as confirmed by examining specimens in the extrusion (i.e., machine) direction. Machine direction views of resulting fibrous blends are shown in Fig. 6a and b for $N=12$. The fibers increased in abundance with continuing processing as the morphology transitions were completed.

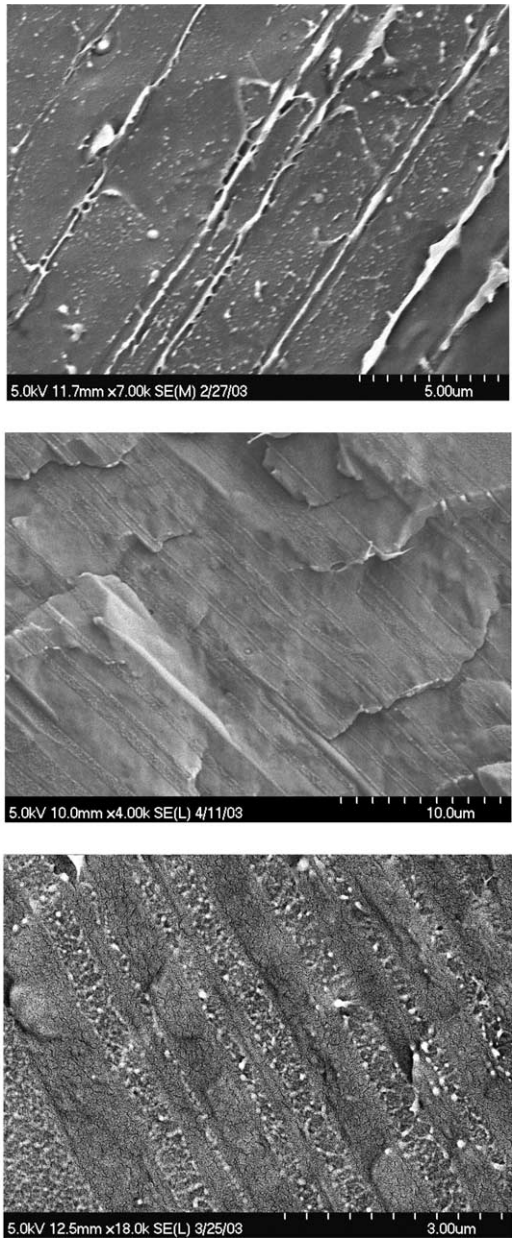

Fig. 4. Comparison of multi-layer morphologies in transverse views in extruded 500 μm films at $N=8$ and for LDPE volume compositions of (a) 10%, (b) 20% and (c) 30%.

For the 30% LDPE blend in Fig. 5c, separation distances between the parent PP layers and LDPE layers in Fig. 4c were smaller. As such, greater opportunity existed for layer interactions. Hole formation in a layer of one polymer component was accompanied by coalescence of adjacent layers of the other polymer component. Layer coalescence was evident in Fig. 5c where the encapsulated oval domains were remnants of LDPE layers in which adjacent holes formed and enlarged. Hole growth in layers of one polymer component was accompanied by melt drainage from adjacent layers of the other polymer component. Melt drainage led to layer thinning and promoted the formation of holes in the adjacent layers. The multi-layer melt of Fig. 4c with $N=8$ was eventually converted volumetrically to an interpenetrating blend for $N=12$. Cryogenic fracture surfaces of films with the interpenetrating blend morphology are shown in the machine direction in Fig. 6c and in the transverse direction in Fig. 7. With $1.4<C_{\mu}<1.7$, the formation of an interpenetrating blend at the low 30% LDPE composition is novel. Droplet morphologies are typically reported in PP based blends at similar minor component concentrations where conventional blending techniques are used. As will be shown, the interpenetrating blend morphology was transitory and convertible ultimately to a

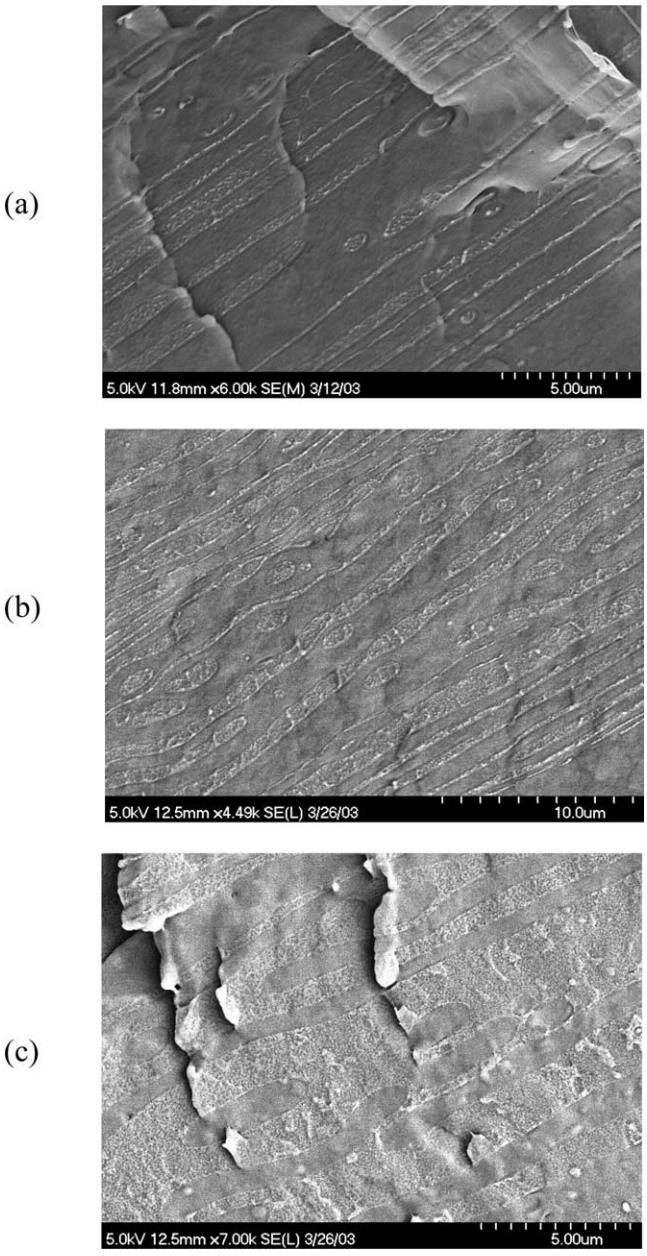

Fig. 5. Morphology transitions in multi-layer morphologies viewed in the transverse direction at $N=10$ for 500 μm films at (a) 10%, (b) 20%, and (c) 30% by volume LDPE.

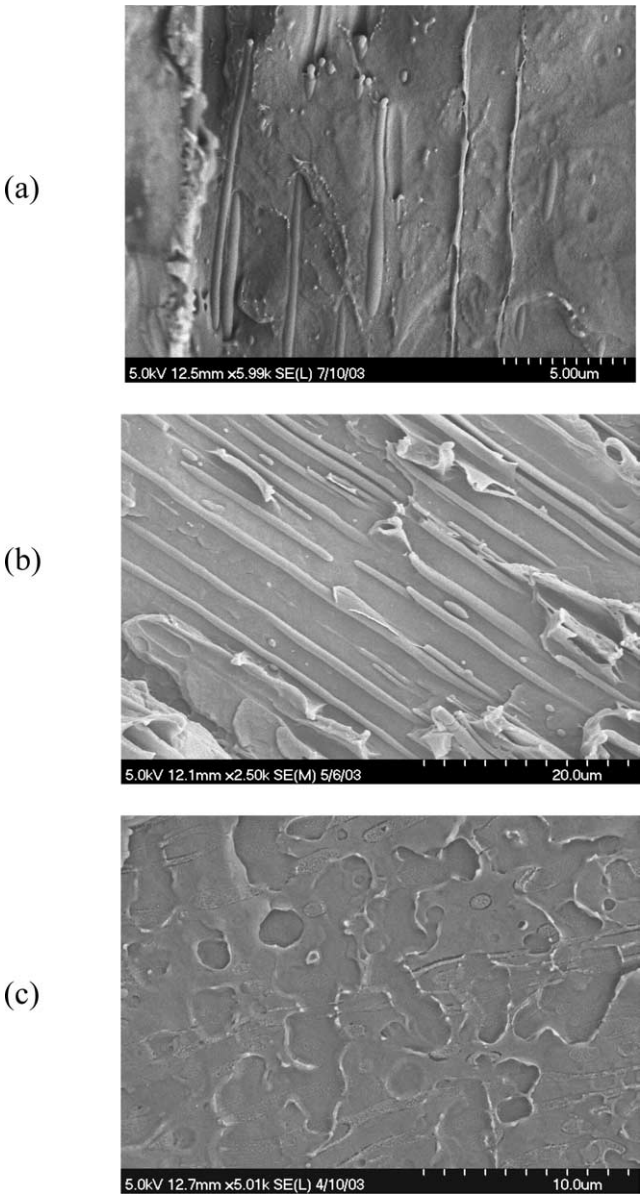

Fig. 6. Comparison of morphologies in machine direction views for 500 μm films at $N=12$ for (a) 10%, (b) 20%, and (c) 30% by volume LDPE. At the lower compositions, thin LDPE layers were converted to long fibers. At 30% LDPE, a dual phase continuous morphology arose via coalescence of alternating layers through layer ruptures.

droplet dispersion. The actual minimum LDPE composition to form an interpenetrating blend with the CCAB was not a focus of this study but may be lower than the 30% value of Fig. 7. The formation of interpenetrating blends via this route was first documented with batch chaotic advection blenders [6–8] but was found also applicable here for the analogous continuous process.

Computational simulations by a lattice Boltzmann method (LBM) have clarified how fibers and the interpenetrating blend in Fig. 6 derive from holes in layers [34]. Regarding fibers, shear causes directional coalescence among adjacent holes in a layer. Interfacial tension and pinch-off of lateral connections subsequently forms coalesced bodies into a circular fiber. Fiber diameters are directly related to parent layer thicknesses. Simulations also have shown an interplay between viscosity ratio and shear level. For higher viscosity ratios, minor component layers with holes are less readily deformed by shear forces so higher shear rates are required to obtain fibers. At intermediate compositions, hole formation occurred in layers of both polymer components due to their similar thicknesses so that a multi-layer morphology was directly converted to one having dual phase continuity such as in Fig. 6c. Good qualitative agreement between modeling and

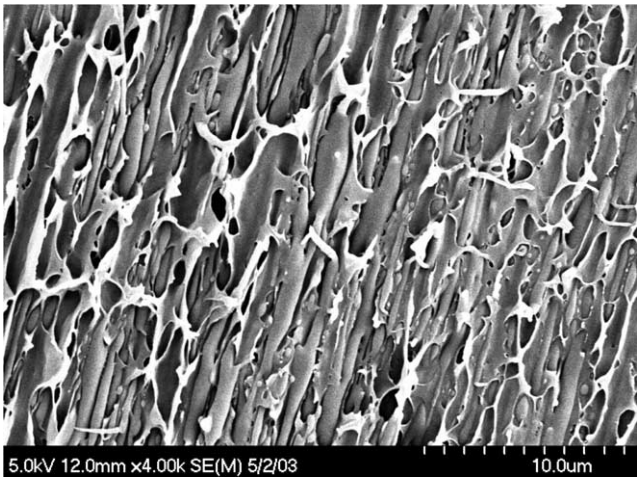

Fig. 7. Transverse view of the interpenetrating blend morphology of Fig. 6. The parent layered morphology is evident.

experiments suggests that blending methods of this study are conducive to simulation. By organizing melts into multiple layers in response to flow fields much simpler than those in conventional blending equipment, blend morphology development is simplified and more readily modeled.

Blends are shown in Fig. 8 for $N=14$ that have morphologies similar to those of the blends produced in Fig. 6 for $N=12$ and correspondingly smaller amounts of cumulative shear. The fibrous and interpenetrating blend morphologies in Fig. 6 were persistent even upon substantial additional shear deformation and a residence time in the CCAB longer by 2 min. This result has special importance in consideration of interest to improve the mechanical properties of injection molded parts by using structured immiscible polymer blends. However, the use of immiscible polymer blends in injection molding raises concerns about beneficial or detrimental morphology changes occurring during melt transfer and melt residence time in molds. For example, LDPE droplets in polystyrene-LDPE blends have become extended by shear deformation to fiber shapes in the near-wall regions of injection molded parts [23]. Improved impact toughness was attributed to the localized fiber structure in the skin region in lieu of a coarsened droplet morphology resulting in the core. Progressive morphology development and operating principles of CCABs (Sections 2.1 and 2.2) suggest that desired blend morphologies may be produced in a CCAB-type device and retained in an injection molded part. For example, if the fibrous morphology of Fig. 6b is desired, the parent multi-layer melt of Fig. 5b might be injected into the mold so that fiber formation would occur upon melt transfer. For injection molding and other purposes, methods of this study permit the dynamic control of blend morphology so that specific blend morphologies can be produced in anticipation of melt transfer steps. These aspects are further discussed in Section 3.2.

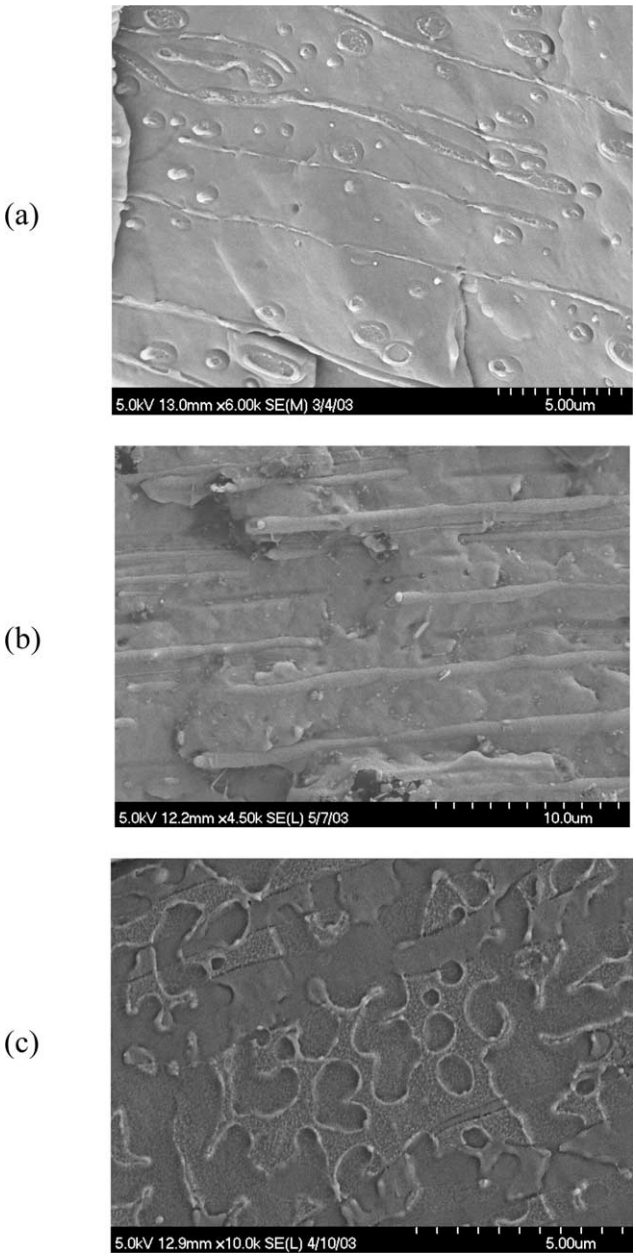

Fig. 8. Stability of blend morphologies of Fig. 6 in response to continued stir rod motion ($N=14$) for (a) 10% (b) 20% and (c) 30% by volume LDPE in PP. This result suggests that resulting blend morphologies may be successfully retained in injection molded parts.

Due to the low concentration of LDPE, the interpenetrating blend morphologies of Figs. 6(c), 7, and 8c were persistent but not stable. Continuing processing led to coarsening such that coarsened domains became subject again to the stretching and folding characteristic of chaotic advection (Fig. 1). The domains yielded new layers or ribbons and platelets. An example of a platelet-ribbon blend morphology is given in Fig. 9 for $N=16$. This result revealed robustness in chaotic advection blending processes with regard to promoting the formation of shapes having high frontal area such as desired for low permeation plastics.

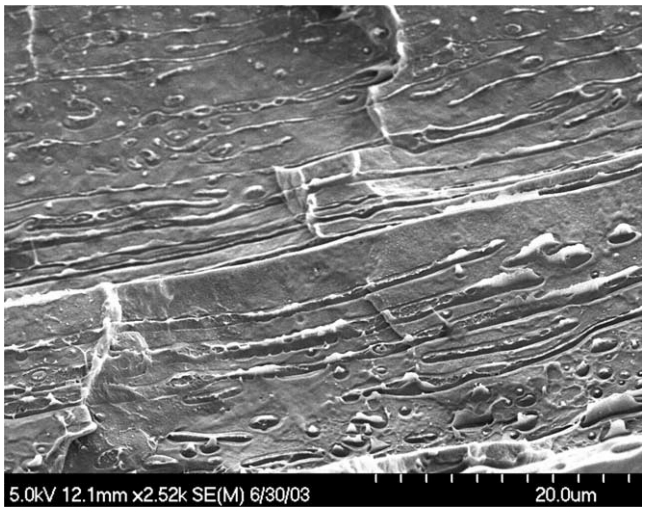

Fig. 9. Platelets, fibers, and droplets for $N=16$ shown in the transverse direction and resulting from the breakup of the interpenetrating blend morphology of Figs. 6 and 7.

An interesting oscillatory morphology development was also identified by this result, where injected melts were converted to layers that underwent morphology transitions giving very different shapes but which coalesced to once again yield layers. The subsequent layers had smaller spatial extents having been derived from earlier layer breakup. As such, their breakup led to droplets. The fibers of Fig. 6 for the 10 and 20% LDPE blends fragmented directly in response to continued processing to also yield droplets. Droplet dispersions for each of the LDPE compositions are shown in Fig. 10 for $N=20$. Droplet diameters at all compositions were in the range of 0.5–1.2 μm. Droplet dispersions with similar droplet sizes were also observed at $N=18$ for the 10% and 20% LDPE compositions, indicating that coarsening occurred slowly. The effect of viscosity ratio in the range 0.8–30 has been systematically studied for PP-polyamide 6 blends produced with a batch chaotic advection blender [36]. Droplet sizes were larger and droplet size distributions were broader for the higher viscosity ratios. Minor component bodies were stretched and folded into multiple layers even at higher viscosity ratios to eventually give droplets. This related study and earlier studies [4,8,10] indicate that a CCAB can be effective in producing droplet dispersions in addition to other blend morphologies even for polymer combinations having adverse viscosity ratios.

3.2. Reproducibility, morphology uniformity, and demonstration of on-line morphology control

Reproducibility of the developed morphologies was assessed by operating the CCAB several weeks later to again produce the blends having 20% and 30% LDPE compositions. Morphologies were in excellent agreement with those obtained earlier. Morphology uniformity was also assessed by examining film cross-sections at three

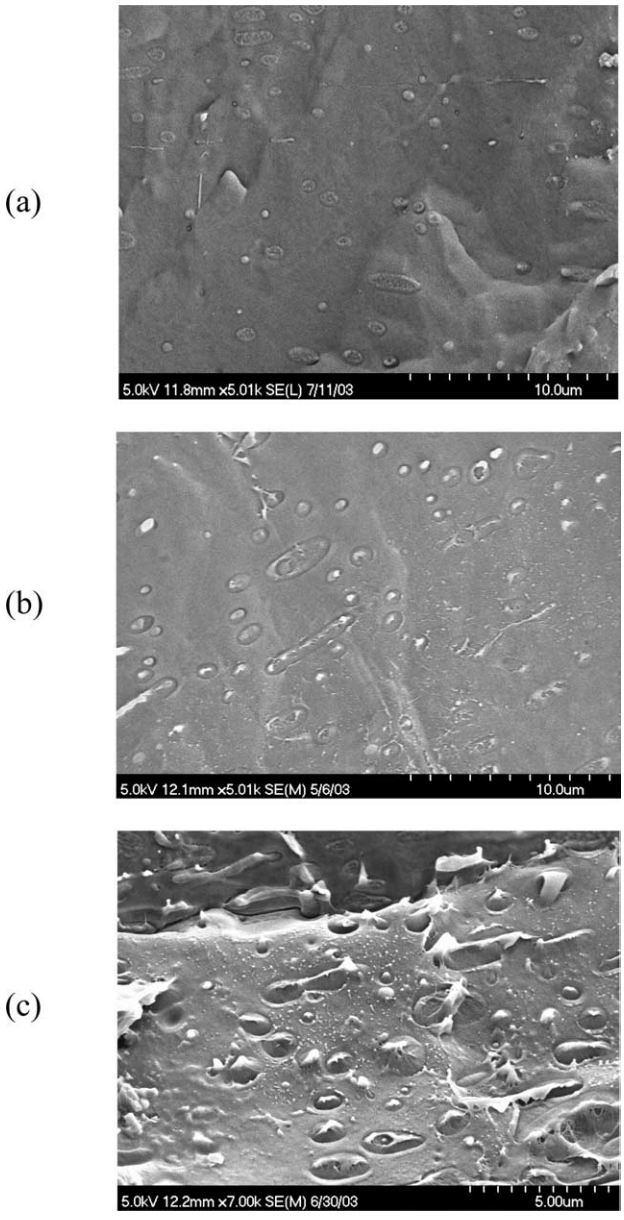

Fig. 10. Droplets formed at $N=20$ for (a) 10%, (b) 20% and (c) 30% LDPE in PP.

distinct locations (i.e., center, off-center, and near edge) in both the transverse and machine directions. Excellent uniformity was observed. The effect of the extrusion step on morphology in the films was also assessed by comparing morphologies obtained with the two film dies of different gap widths (i.e., 150 or 500 μm). The sequence of morphologies was identical with both dies although the 150 μm die provided derivative morphologies at a lower N. The N values for a particular morphology with each die were related by $N_{500} \approx N_{150} + 2$.

The comparative result above with dies of different gap width indicated that a portion of the morphology development occurred in the die. However, because of progressive morphology development, operation of the CCAB can be

controlled to deliver a particular blend morphology either to the die inlet or die exit. This ability to dynamically control blend morphology is demonstrated in Fig. 11 for the 30% LDPE composition. The blend morphologies in Fig. 11 were generated by selectively altering the melt residence time in the CCAB with no disruption in its operation. For the micrograph sequence $N=8$, 12, and 14, melt residence time was continuously increased so that a multi-layer morphology led sequentially within a single extrusion to an interpenetrating blend and to a blend consisting of ribbons and platelets. Morphology development within the CCAB of Fig. 1 occurred as melt moved along the stir rods toward the extrusion point. However, by reducing the rod speed or increasing the extrusion rate, morphology development can be slowed. For the micrograph sequence $N=14$, 13, and 9, melt residence time was continuously decreased so that the morphology development was reversed from the sequence $N=8$, 12, and 14. This novel ability to dynamically control blend morphology makes possible the production of extrusions with graduated or periodic morphologies. It also can allow on-line optimization of properties when implemented together with a suitable measurement method. With respect to injection molding, a CCAB can be controlled to deliver a blend morphology such that subsequent morphology transitions that may occur during melt transfer or solidification steps yield a product with favorable overall properties.

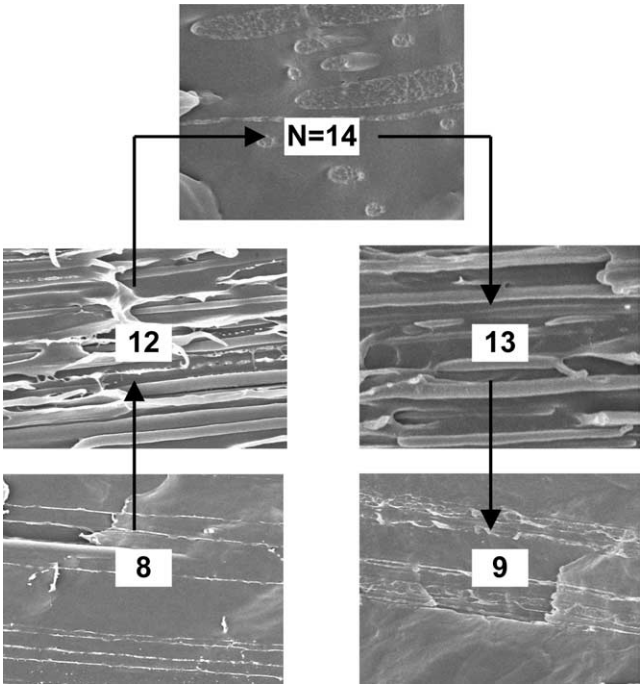

Fig. 11. Example of novel on-line control of morphology development in extrusions by the dynamic operating mode. From the perspective of the die, intermediate morphologies are obtainable in repeatable forward and reverse sequences by decreasing or increasing the rod rotational speed and thereby changing the amount of in situ structuring occurring. The case shown pertains to the 30% LDPE blend extruded with the 150 μm die.

3.3. Tensile and impact toughness properties

When blends are produced with screw extruders, droplet dispersions are typically obtained at the low LDPE compositions of this study. As such, many of the blend morphologies of Figs. 4–9 are novel and their mechanical properties have not been previously reported. Because chaotic advection in the CCAB (Fig. 1) redistributed the injected melts from the melt distribution block and also in tandem formed them into shapes of smaller sizes, morphology and compositional variability was larger for films produced with small N. Mechanical properties of film specimens taken from these films had resulting larger standard deviations. Standard deviations reduced in tandem with improvements in compositional uniformity and blend feature size reductions as N increased. The percentage standard deviations are given in Table 1. Values for other N can be estimated by linear interpolation. Standard deviations for $N>2$ were similar to those reported in blending studies where conventional compounding equipment is used. These small standard deviations were consistent with excellent morphology uniformity described in Section 3.2.

Morphological effects on ultimate tensile strength and tensile modulus in the machine direction for films with 20% and 30% LDPE are shown in Fig. 12 in terms of N. Corresponding blend morphologies for each N are shown in prior figures. The properties of PP films also produced with the CCAB are indicated for comparison. Tensile strength increased as the number of layers in the multi-layer morphology became more numerous and the layers became correspondingly thinner. A peak strength occurred in the 20% LDPE blend at $N=6$ and in the 30% LDPE blend at $N=5$. Tensile modulus increased similarly. Layer breakup such as shown in Fig. 5 for $N=10$ resulted in abrupt decreases in modulus for both the 20% and 30% LDPE blends. The spongy, interpenetrating blend morphology of Figs. 6(c), 7, and 8c for the 30% LDPE blends that pertained to $10<N<14$ caused a marked increase in the machine direction strength within this N interval. Its fragmentation at higher N and conversion to the ribbon-platelet morphology of Fig. 9 at $N=16$ and subsequently to a droplet dispersion for $N>18$ (Fig. 10) led to a decline in tensile strength. Similar results in Fig. 13 were obtained for film specimens taken in the transverse direction with the exception that the interpenetrating blend morphology ($10<N<14$) caused a marked reduction in modulus and no discernible increase in strength. The directional characteristics of the interpenetrating blend morphology that are evident in Fig. 7 may provide an explanation. It should be noted that the interpenetrating morphology was incipient. Less directionality might arise at a higher LDPE composition such that LDPE interconnections would be less tenuous. Interestingly, morphology types other than the common droplet morphology ($N>18$) provided better performance in Fig. 12 in terms of tensile strength and modulus. Because droplet morphologies typify PP-LDPE blends currently produced at these LDPE

Table 1
Percentage standard deviations in tensile and impact toughness measurements. Values decreased monotonically as LDPE domains became better distributed and simultaneously refined by chaotic advection

N	Modulus (80/20)	Modulus (70/30)	Strength (80/20)	Strength (70/30)	Toughness (80/20)	Toughness (70/30)
2	7.3	13.3	13.2	38.0	1.6	2.3
10	2.9	9.2	4.7	3.5	1.3	1.4
19	1.4	1.8	2.1	2.4	0.9	1.1

compositions as well as many other blends with low minor component compositions, this result suggests that other morphology types may be more desirable where tensile properties are an important consideration. In Fig. 12, tensile strength and tensile modulus with $N=6$ for the 80/20 blend were increased by 15% and 26% relative to the values for the droplet morphology at $N=19$. Increases also arose for the 70/30 blends but were smaller.

Impact toughnesses depended strongly on blend morphology. In Fig. 14 for $N<5$, changes to impact toughness were small. However, for $N=5$, impact toughness increased in response to greater compositional uniformity and reductions in layer thicknesses. Multi-layered structures in polymer blends have been previously reported to enhance toughness. For example, in polycarbonate-styrene acrylonitrile blends having multi-layer morphologies, toughness increases were attributed to changes in crazing behavior and the generation of craze arrays as layers became thin [37]. Using a batch chaotic advection blender, the impact properties of PS were similarly enhanced by forming LDPE into layers [5]. The more readily deformable LDPE layers mitigated stresses imposed on PS layers during impact. In the 20% LDPE blends, numerous LDPE layers in Fig. 4b had thicknesses in the range of 0.5–1.5 μ. The multilayer morphology with $N=6$ for the 20% LDPE blend provided continuity for stress transfer and exhibited

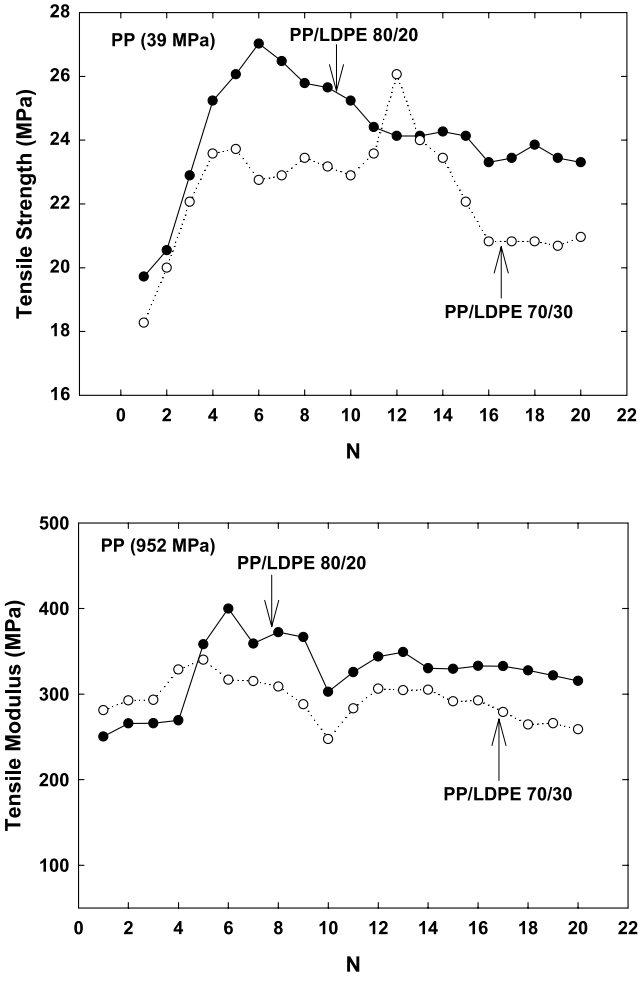

Fig. 12. Effect of composition and morphology on (a) ultimate tensile strength and (b) modulus of PP/LDPE blends in the machine direction.

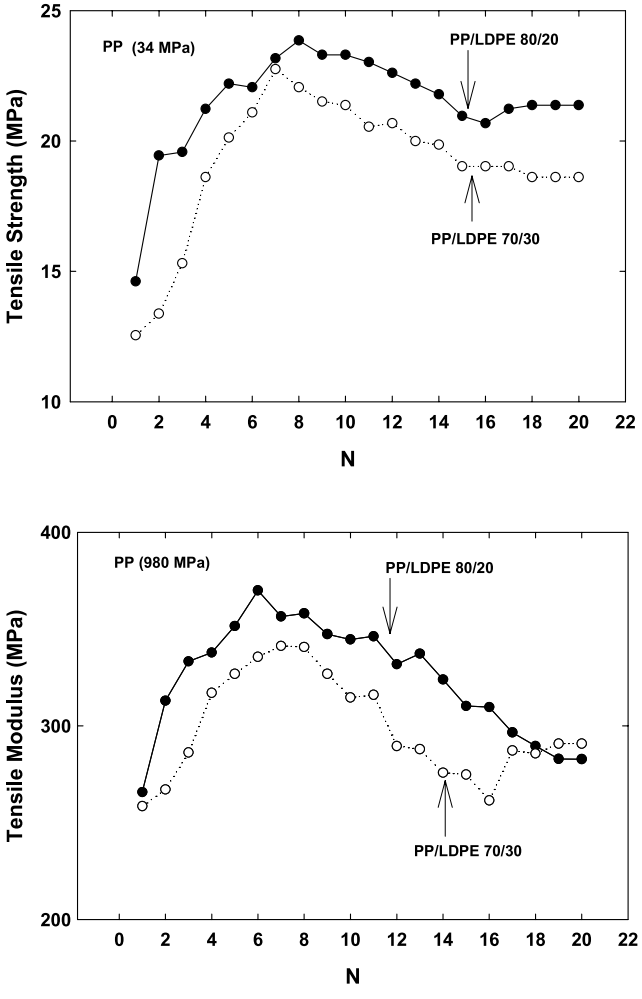

Fig. 13. Effect of composition and morphology on (a) ultimate tensile strength and (b) modulus of PP/LDPE blends in the transverse direction.

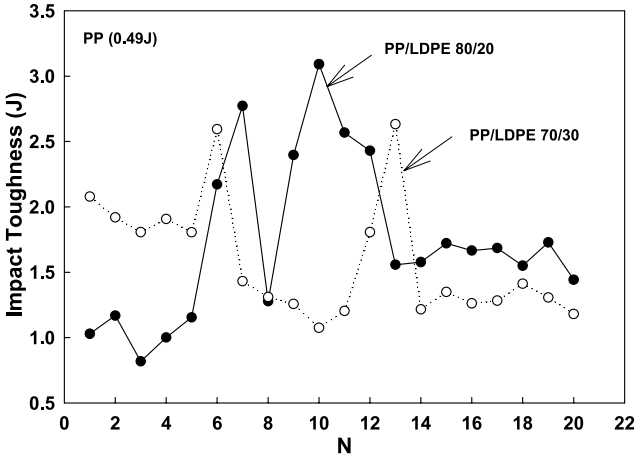

Fig. 14. Influences of morphology on impact toughnesses of PP/LDPE blends.

enhanced ultimate tensile strength relative to the corresponding droplet morphology at $N>16$. For $N=6$ for the 20% LDPE blend and $N=7$ for the 30% LDPE blend, impact toughness abruptly decreased. These decreases were related to the initial breakup of LDPE layers and also accompanied decreases in machine direction modulus in Fig. 12. Structurally, ruptures in LDPE layers became filled with PP such that the thicknesses of PP layers were reduced and shear stresses in them became correspondingly increased. Increased localized stresses in the vicinities of layer ruptures may have also contributed to smaller toughnesses in comparison to the multi-layer case. It is interesting to note that toughnesses were similar to the value for droplets ($N>18$) where stress concentrations can also arise. The peak impact toughness for the 20% LDPE films was obtained for $N\approx 9.5$ for a blend consisting of LDPE layers and fibers such as shown in Fig. 5b. For blends produced at higher N, progressive morphology development led to an increasing population of fibers at the expense of layers from which they were formed. The fibers in turn yielded droplets. As such, the peak impact toughness reduced to the impact toughness associated with droplets for $N>18$. The peak impact toughness of the 30% LDPE films was obtained for $N=10$ due to the interpenetrating blend (Fig. 7). Because it was formed at a low LDPE composition, melts processed with $N>14$ did not retain the interpenetrating blend morphology as discussed in Section 3.1. The interpenetrating morphology was converted to a mixture of platelets and ribbons (Fig. 9) and ultimately droplets (Fig. 10). Impact toughnesses reduced in concert. Quantitatively, for the 20% LDPE blends with $N=10$, a 96% improvement in impact toughness relative was obtained relative to the value for the droplet morphology and a 550% increase relative to the value for PP. For the 30% LDPE blends, impact toughness was improved by 93% relative to the value for the droplet morphology and by 430% relative to the value for PP.

In addition to the mechanical properties documented in Figs. 12–14, delamination of layers within an extruded film is also an important concern. Delamination can be problematic due to poor interfacial adhesion resulting when multi-layer films are formed from immiscible polymers, typically by co-extrusion. Incorporation of a compatibilizer in PP-LDPE blends is widely considered an imperative due to incompatibility and a need to improve interfacial strength. For the PP-LDPE films produced with the CCAB, delamination did not occur even subsequent to tensile and impact tests. Delamination was prevented for the multi-layer morphologies since each polymer component was stretched and folded about the other by chaotic advection. Delamination was prevented for other layered morphologies due to interconnections among layers at layer rupture locations. Morphologies were also produced that were continuous in the PP phase while still containing LDPE bodies of high frontal area (Fig. 9). All such morphologies can find application to barrier plastics [12].

4. Conclusions

Although a new technology awaiting further development, a unique continuous chaotic advection blender (Fig. 1) provided a variety of blend morphologies at constant compositions. Blend morphologies reported in earlier studies with batch chaotic advection blenders were also producible in the more industrially relevant continuous flow mode and were retained in extrusions. This in situ structuring method differed substantially from conventional blending methods where blend morphology is a consequence of mixing in lieu of deliberate melt manipulation. Morphology development in the CCAB progressed as melt flowed toward the extrusion point. Chaotic advection converted injected melt streams by its characteristic stretching and folding into multiple layers. Melt components were also distributed among one another to yield greater compositional uniformity at smaller length scales. Layer breakup yielded blends having interconnected layers, dual phase continuous structures (i.e., interpenetrating blends), fibers, platelets, ribbons, and droplets. An oscillatory morphology development was also identified whereby injected melt streams are converted to layers which yielded breakup bodies or coalesced layers that are again converted to thin layers by chaotic advection. Robustness in forming layered morphologies in CCAB devices was indicated. With regard to mechanical properties, the droplet morphology that is typically obtained with conventional blending equipment provided tensile strength, tensile modulus, and impact toughness smaller than several of the novel blend morphologies produced. In particular, for the 20% LDPE blends, a blend consisting of numerous thin layers, layers interconnected via holes, and fibers provided a 96% improvement in impact toughness relative to the value for the droplet morphology and a 550% increase relative to the value for PP. Tensile modulus and tensile strength were

also improved in comparison to values pertaining to the droplet morphology. Processing methods made possible the selection of a blend morphology having a combination of desirable properties. Operation in a continuous mode provided novel process control capabilities. Particular blend morphologies were producible through specification of the amount of melt structuring imposed by stir rods while melt was resident in the CCAB. Dynamic control was possible such that extrusions can be produced with graduated or periodically varying blend morphologies along their lengths. An ability to control blend morphology on-line can allow rapid property-composition optimization and also may make possible the production of functional plastic materials such as those having selective permeability or directional electrical properties. With regard to injection molding, results suggest that a CCAB can be controlled to deliver a blend morphology such that subsequent morphology transitions that may occur during melt transfer or solidification steps yield a product with favorable overall properties. The progression of morphology development as melt flowed within the CCAB barrel also suggests successful transport of structured melts in molds is possible.

Acknowledgements

Financial support was provided by the Engineering Research Center Program of the National Science Foundation under Award No. EEC-9731680 and by the Dow Chemical Company. The authors express their appreciation to M.D. Read of Dow.

References

[1] Aref H. J Fluid Mech 1984;143:1.
[2] Aref H. Phys Fluids 2002;14:1315.
[3] Zumbrunnen DA, Miles KC, Liu YH. Composites, Part A 1996;27A: 37.
[4] Liu YH, Zumbrunnen DA. Polym Compos 1996;17:187.
[5] Liu YH, Zumbrunnen DA. J Mater Sci 1999;34:1701.
[6] Zumbrunnen DA. J Text Inst 2000;3:92.
[7] Kwon O, Zumbrunnen DA. J Appl Polym Sci 2001;82:1569.
[8] Zumbrunnen DA, Chhibber C. Polymer 2002;43:3267.
[9] Zumbrunnen DA, Inamdar S. Chem Eng Sci 2001;56:3893.
[10] Zumbrunnen DA, Inamdar S, Kwon O, Verma P. Nano Lett 2002;2: 1143.
[11] Ottino JM, Muzzio FJ, Tjahjadi M, Franjione JG, Jana SC, Kusch HA. Science 1992;257:754.
[12] Kwon O, Zumbrunnen DA. Polym Eng Sci 2003;43:1443.
[13] Baer E. Sci Am 1986;255:179.
[14] Li J, Shanks RA, Long Y. J Appl Polym Sci 2000;76:1151.
[15] Liang JZ, Li RKY. J Appl Polym Sci 2000;77:409.
[16] Tam WY, Cheung T, Li RKY. Polym Testing 1996;15:363.
[17] Yokoyama Y, Ricco T. Polymer 1998;39:3675.
[18] Jafari SH, Gupta AK. J Appl Polym Sci 2000;78:962.
[19] Tai CM, Li RKY, Ng CN. Polym Testing 2000;19:143.
[20] Teh JW. J Appl Polym Sci 1983;28:605.
[21] Galeski A, Pracella M, Martuscelli E. J Polym Sci, Polym Phys 1984; 22:739.
[22] Ramsteiner F, Kanig G, Heckmann W, Gruber W. Polymer 1983;24: 365.
[23] Teh JW, Rudin A. Polym Eng Sci 1991;31:1033.
[24] Chiu W, Fang S. J Appl Polym Sci 1985;30:1473.
[25] Lu J, Wei GX, Sue HJ, Chu J. J Appl Polym Sci 2000;76:311.
[26] Miles KC, Nagarajan B, Zumbrunnen DA. J Fluid Eng 1995;117:582.
[27] Gomillion B. PhD Thesis. Clemson University; 2000.
[28] Aref H, El Naschie MS. Chaos Solitons Fractals 1994;4:745.
[29] Khakar DV, Rising H, Ottino JM. J Fluid Mech 1986;172:419.
[30] Leong CW, Ottino JM. J Fluid Mech 1989;209:463.
[31] Kusch HA, Ottino JM. J Fluid Mech 1992;236:319.
[32] Ramaswami S. MS Thesis. Clemson University; 2005.
[33] Zhang DF, Zumbrunnen DA. J Fluid Eng 1996;118:40.
[34] Joshi A, Zumbrunnen DA. Chem Engrg Comm (in press).
[35] Sundararaj U, Dori Y, Macosko CW. Polymer 1995;36:1957.
[36] Jana SC, Sau M. Polymer 2004;45:1665.
[37] Haderski D, Sung K, Im J, Hiltner A, Baer E. J. Appl Polym Sci 1994; 52:121.